Proceedings of the Twenty-first (2011) International Offshore and Polar Engineering Conference
Maui, Hawaii, USA, June 19-24, 2011

ISBN 978-1-880653-96-8 (Set); ISSN 1098-6189 (Set); www.isope.org

Numerical Study on Nonlinear Hydroelastic and Hydrodynamic Effects on Floating Body Using Eulerian Scheme with Lagrangian Particles

Suandar Baso, Hidemi Mutsuda, Kenta Kawakami, Kouichi Hashihira, Yasuaki Doi
Department of Social and Environmental Engineering, Graduate School of Engineering, Hiroshima University
Higashi Hiroshima, Hiroshima, Japan

ABSTRACT

Ship motions with water impact have been extensively devoted to solve toward viable solution by using a lot of techniques. This study deals with a design tool using CFD and criteria for a ship structure with elasticity under impact pressure loads due to slamming, green water and sloshing in waves. In this study, our numerical model which combines an Eulerian scheme with Lagrangian particles has been enhanced directly for predicting nonlinear hydroelastic and hydrodynamic effects on a floating body in waves. The proposed model can treat and solve simultaneously both nonlinear fluid and floating body motions with elasticity. Firstly, the enhanced numerical model was performed on a water entry problem of a rectangular body with elasticity to verify accuracy and usefulness of our numerical model. The computed strain and stress caused by nonlinear hydroelastic during water entry process were in good agreement with experimental results. Next, the proposed model has been applied to hydroelastic response caused by ship slamming in waves.

KEY WORDS: Water impact; ship slamming; hydroelasticity; grid based method; particle based method

INTRODUCTION

A ship as massive sea transportation is not really a rigid body. When hydrodynamic loads due to slamming occur on a time scale of important structural periods, hydroelasticity should be considered. This is reasonable that it can suffer impact pressure and vibration influencing ship performance, ship structure and passenger comfort caused by strongly interaction wave-ship. Therefore, wave induced hydrodynamic and hydroelastic response on a ship body has to be important consideration and requirement in a ship design to guarantee a ship navigation at sea.

The developments of Computational Fluid Dynamics (CFD) techniques to predict accurately hydrodynamic and hydroelastic effects on floating bodies need tremendous efforts. These are indicated that some numerical approaches and experimental works for prediction of water impact with free surface flows in various forms and techniques, by beginning with the research results of von Karman (1929) and Wagner (1932), have been investigated e.g. a series of photographs of cylinder's entry to and exit from water surface and time dependent water entry for wedges of various angles with both gravity and non-linear boundary conditions (Greenhow and Lin, 1983; Greenhow, 1987), Experiment with the impact of surface planes on still water and identification of the entrained air effect between free surface and the body (Chuang, 1967), a comparison of the maximum impact pressure of a symmetrical wedge between experimental data and several numerical results (Engle and Lewis, 2003), and slamming loads on two-dimensional symmetric section based on Boundary Element Method and extension method to general asymmetric bodies and comparison validation with experiment of a wedge and a bow flare section (Zhao and Faltinsen,1993; Zhao et al., 1997). The effect of flow separation for axisymetric impact was also investigated by Zhao and Faltinsen (1998). However, all numerical investigations presented that the fluid has irrotational and inviscid flow and these cannot adequately handle flow with water impact involving plugging waves and air bubbles.

Moreover, several numerical methods which governed the Navier-Stokes equation with free surface capturing have been presented; the application of a volume of fluid method (VOF) for solving two-density fluid (Ng and Kot, 1992; Hirt and Nichols, 1981), numerical study of water impact on cylindrical shell and a bow flare section using a Euler equation and VOF method (Arai et al., 1994 and 1998), application to bow flare slamming by varying flare angles (Schumann, 1998), numerical results of water entry of a wedges, a cylinder and a cone into calm water using VOF method with a local height function (Kleefsman et al., 2005), water entry problems solved by using Smoothed Particle Hydrodynamic (SPH) method (Gingold and Monaghan, 1977; Landrini et al., 2001; Oger et al., 2006). Deuff et al. (2006) proposed the coupled SPH-SPH fluid structure scheme and also applied to the water entry of a V-shaped wedge for investigating hydrodynamic impact. However, the hydroelastic effects caused by trapped air, air cushion and water flow response on an elastic body are phenomena that are difficult to solve more clearly. Therefore, hydroelastic effects caused by interaction fluid-structure cannot be neglected because structures have a response with respect to water behaviors, vice versa.

In applications to ship slamming, some researchers have predicted and clarified slamming behaviors on a ship more extensively. The term of hydroelasticity was stated clearly by Faltinsen (1997 and 1998). The hydroelastic formulation and model slamming was investigated by Bereznitski et al. using numerical model (2001a, 2001b, 2001), Tajima and Yabe (1999) was simulated a vessel slamming by using CIP method. Kvalsvold et al. (1995) studied wave impact on elastic beams. Then, Faltinsen (1999) presented water entry of a wedge by hydroelastic orthotropic plate theory and an approximate three-dimensional theoretical investigation of hydroelastic wetdeck slamming, and also presented a theoretical study of representing the wetdeck as a beam model and accounting for dynamic hydroelastic effects (Faltinsen et al., 1997, Faltinsen, 2001, Bereznitski et al., 2000). Although there are several simulation tools that can predict water impact due to strongly nonlinear wave-body interactions, yet there are several remaining difficulties in calculating water impact associated with highly nonlinear free surface, and also its accuracy is currently confined in reproducing and validating.

In our previous works, our numerical method was applied successfully and accurately to seakeeping performace and resistance in calm water and nonlinear waves with breaking for several kinds of ship types and Froude numbers. In recent work using our numerical method, a coupled Eulerian scheme with Lagrangian particles (Mutsuda et al., 2007, 2008, 2009a, 2009b, 2010) which combines CIP method (Yabe and Wang, 1991) and SPH method (Gingold and Monaghan, 1977), has been developed continually to verify its usefulness in a design process to predict impact pressure with free surface flow caused by nonlinear interaction between wave and ship motions. The model has two kinds of Lagrangian particles, i.e. SPH and free surface particle, on Eulerian grids to correct interface tracking error. The two types of Lagrange particles are collocated and attracted with highly accurate captured free surface under resolved region with Eulerian grids. Interaction between movable and a deformable ship body with fluid flows, as fluid-structure interaction problems, is solved by acceleration obtained from the pressure on the SPH particles interpolated using pressure on grids. Then, the internal stress and strain are induced in a ship body caused by impact pressure and the elastic movement. Using SPH particles which represent a ship body, the internal stress and strain can be captured clearly as well.

In this study, the developed numerical method has been performed firstly on application to the water entry problems of a rectangular body with elasticity to verify and validate its accuracy and usefulness. Then, it has been applied to hydroelasticity, internal stress and strain response due to impact pressure caused by a ship slamming in waves. Finally, we conclude that the present model is a powerful tool to be capable of computing a strongly nonlinear hydroelastic response between wave and a ship.

COMPUTATIONAL METHOD

In this section, the numerical method, which combines the Eulerian scheme and the Lagrangian particles by coupling the SPH method and CIP method with particle, are described concisely. More detail explanations were stated in the previous publication (Baso et al., 2010). First, the CIP method with particles is introduced as a numerical scheme that combines the accuracy of Lagragian front tracking. Thereafter, the SPH method is employed to calculate deformation, strain, stress of elastic body, and 3D motion.

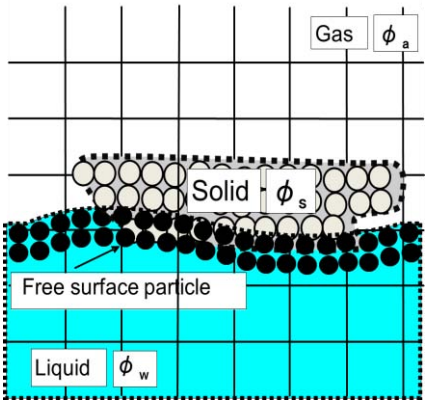

Fig.1 Illustration of the proposed model (ϕ_I indicates density function; Lagrangian particles are located on Eulerian grid)

Eulerian Scheme with Lagrangian Particles

Arrangement of grids and particles

The developed Eulerian scheme with Lagrangian particles has been illustrated as shown in Fig.1. This scheme uses a staggered grid system and has two types of Lagrange particles, i.e. SPH particles to describe solid and free surface particles to capture free surface accurately.

Density function ϕ_I defined on a grid node is corrected by using density function ϕ_P on free surface particles within referenced area with radius h. A smooth approximation of a density function can be constructed by using a Kernel function in the SPH method.

Governing equations for fluid phase

The governing equations for fluid phase consist of the mass conservation equation, incompressible Navier-Stokes equation and the equation of continuity, I-phase density function ϕ_I ($0 \le \phi_I \le 1$) and its advection equation. The equations are expressed as follows:

$$\frac{\partial \bar{u}_i}{\partial x_i} = 0 \tag{1}$$

$$\frac{\partial \bar{u}_i}{\partial t} + \bar{u}_j \frac{\partial \bar{u}_i}{\partial x_j} = -\frac{1}{\rho}\frac{\partial \bar{P}}{\partial x_i} - \frac{\partial \tau_{ij}}{\partial x_j} + \frac{\mu}{\rho}\frac{\partial^2 \bar{u}_i}{\partial x_j \partial x_j} + g_i + \bar{F}_{fsi} \tag{2}$$

$$\frac{\partial \phi_I}{\partial t} + \bar{u}_j \frac{\partial \phi_I}{\partial x_j} = 0 \tag{3}$$

where, u_i is the velocity, μ the coefficient of fluid viscosity, ρ the fluid density, P the pressure, F_{fsi} the fluid-structure interaction, g_i the acceleration due to garvity, τ_{ij} the SGS stress term, and ϕ_I the density function. To reduce model parameters, the SGS stress term is solved by using the Dynamic SGS model proposed by Germano(1992). More details are provided by Mutsuda and Yasuda (2000).

Advection step and non-advection step

The governing equations are solved by using the splitting method which is suitable for solving a multi-phase flow without smearing a density across interface between air and water. The advection step is calculated by the CIP method proposed by Takewaki and Yabe (1987). Then, the Type-M scheme of the CIP method is employed by using the third-order accuracy in time and space (Yabe et al., 2004). On the other hand, the non-advection step is solved by using the second-order finite difference method.

Governing equations for Solid phase

The governing equations for solid phase are the continuity and momentum equations as follows:

$$\frac{D\rho}{Dt} + \rho \frac{\partial u^i}{\partial x^i} = 0 \tag{4}$$

$$\rho \frac{Du^i}{Dt} = \frac{\partial \sigma^{ij}}{\partial x^j} - F_{fsi} \tag{5}$$

where ρ is the density, u^i the velocity, x^j the position vector of vector j components, σ^{ij} the stress tensor of the solid phase, and F_{fsi} the fluid structure interaction term. The stress tensor σ_s^{ij} in Eq.(5) is given by

$$\sigma_s^{ij} = -P\delta^{ij} + S^{ij} \tag{6}$$

where S^{ij} is the deviatoric stress tensor, $P = -\sigma_{kk}/3$ the pressure solved by the Poisson's equation (9) as mentioned below.

Our numerical model considers a large deformation of an elastoplastic body. The solid body changes at every calculation step by using the following equation:

$$\{dS^{ij}\} = [D^{ep}]\{d\varepsilon^{ij}\} \tag{7}$$

where D^{ep} is the elastoplastic matrix, $d\varepsilon^{ij}$ the time increment of the strain, and dS^{ij} the time increment of the deviatoric stress. To solve rotation of the solid phase during a deformation, the Jaumann derivative is used to ensure material frame indifference with respect to the rotation as follow:

$$\frac{dS^{ij}}{dt} = 2\mu\left(\dot{\varepsilon}^{ij} - \frac{1}{3}\delta_{ij}\dot{\varepsilon}^{ij}\right) + S^{ik}\Omega^{jk} + \Omega^{ik}S^{kj} \tag{8}$$

where $\dot{\varepsilon}$ is the strain rate tensor and Ω the spin tensor. Other details are given by Mutsuda et al. (2009a,b,c).

The pressure with specified jump conditions is solved by the Poisson's equation given by

$$\nabla \cdot \left(\frac{\nabla P^{n+1}}{\rho^*}\right) = \frac{\nabla \cdot u^*}{\Delta t} \tag{9}$$

where $*$ denotes a physical value after the advection step. The pressure for solid phase can be obtained by this equation and be applied in solving a solid deformation.

The fluid structure interaction F_{fsi} is solved by acceleration obtained from the pressure on the SPH particles interpolated using the pressure on grids solved by the Poisson's equation (9). In the model, the fluid structure interaction F_{fsi} in Eqs.(2) and (5) can be given by the following equation:

$$F_{fsi}(\mathbf{r}_a) = -\frac{1}{\rho(\mathbf{r}_a)}\sum_b m_b \frac{P(\mathbf{r}_b)}{\rho(\mathbf{r}_b)}\nabla_a W(\mathbf{r}_a - \mathbf{r}_b, h) \tag{10}$$

To keep computational efficiency and stability, the time increment in the solid phase is approximately 1/10 to 1/50 of that in fluid phase.

Ship Motion

A ship motion is solved by using information obtained from SPH particles because a ship hull consists of SPH particles capturing motion and deformation of a ship. Therefore, the 3D motion of a ship hull is represented by describing translation and rotation of the center of gravity of a ship hull by using the following equations:

$$\frac{\partial^2 x_{s,k}}{\partial t^2} = \frac{F_{s,k}}{m_i} - F_{fsi} \tag{11}$$

$$I\frac{\partial \omega_i}{\partial t} = T_i \tag{12}$$

$$\frac{\partial \theta_i}{\partial t} = \omega_i \tag{13}$$

where θ_i is the rotational angle, ω_i the angular velocity, T_i the torque, I the inertia moment, and F_{fsi} the fluid structure interaction. In addition, the center of gravity of a ship hull can be obtained by solving the inertia moment of SPH particles, and this is calculated by using Baraff theory (1997). Therefore, the coordinates of velocity of each SPH particle in every time step can be tracked by using the rotation matrix and the amount of the angle rotation of the center of gravity. The quaternion is also used instead of the rotation matrix $\boldsymbol{R}(t)$ in 3D to avoid the Gimbal lock phenomenon.

RESULTS AND DISCUSSION

Application to Water Entry Problem of Elastic body

Experimental Set Up and Results

Experimental work of a water entry test of elastic body has been performed in the wave tank of Hiroshima University. The purpose is to obtain water impact and hydroelastic response of a rectangular body with elasticity. Here, the experimental setup and device were determined and designed in the basis of the free fall as shown in Fig. 2. The elastic body at initial condition was supported by four-legs framed structure. The pressure, stress and strain are measured by using piezo-electric sensors located on the bottom frame of the elastic body and linked to PC. High speed digital video camera was also placed to visualize the body's motion and to capture the free surface with splashing to analyze using PTV and PIV techniques.

The water impact and the elastic response acting on a rectangular body with a different Young's modulus are measured in water entry experiments. One example of the rectangular model we have used is shown in Fig.3. S1 to S3 means measurement positions of strain. P1 to P3 indicates locations of piezoelectric sensors.

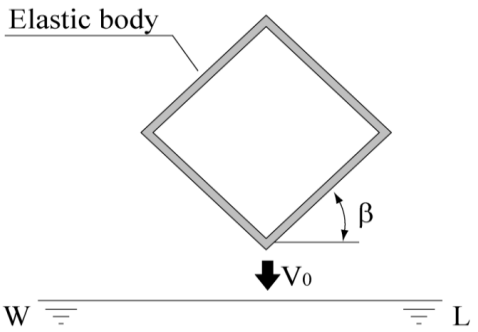

Fig. 2 Experimental setup for water entry problem of elastic body (V_0 : Entry speed, β : Deadrise angle)

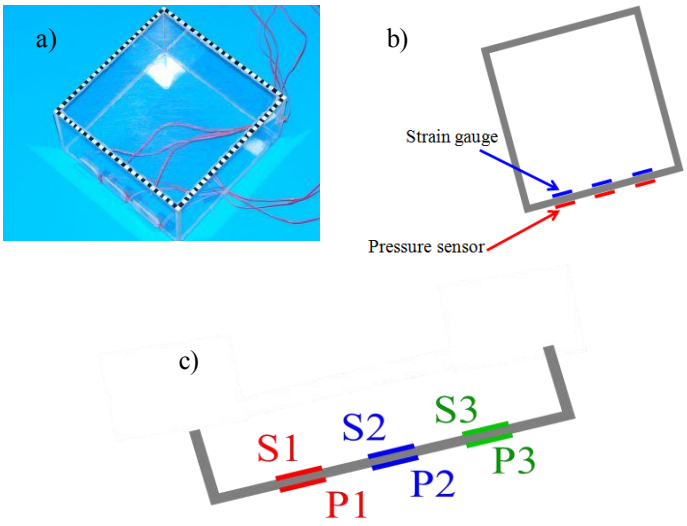

Fig. 3 Experimental model of elastic rectangular structure. The strain gauges S1 ~ S3 and pressure sensors P1 ~ P3 are located on the lower frame of the model.

The elastic models are made of aluminum and acrylic with Young's modulus 6.9×10^8 Nm^{-2} and 3.14×10^8 Nm^{-2}, respectively. The raging deadrise angles β between still water level and the bottom frame of the elastic body were set from zero to 45 degree as shown in Fig. 2.

The dimensions of the elastic models are 8x8x8cm for aluminum type and 20x20x20cm for the acrylic type, and the thickness is 2mm and 5mm, respectively. The dropping speed was 2.8m/s above the free surface.

To investigate relationship between impulsive pressure and deformation of the elastic body, we focused on the acrylic type. The experimental result of impact pressure of the acrylic body was confirmed with experimental results conducted by Chuang as shown in Fig. 4. In Chuang's experiment, the solid body was used. The non-dimensional maximum impact pressure P^{**} is defined by standardized parameter concerning with the piezoelectric sensor. The $P1$ denoted by red dot is lower point, middle point $P2$ is blue dot, and upper point $P3$ is green dot as shown in the previous Fig3. The maximum pressure is increasing with decreasing the deadrise angle β and the impact pressure is suddenly dropping at nearby $\beta = 0$. Tendency of the experimental results shows in consistency with the experimental results by Chuang's data. In Fig. 5, the strain data is decreasing with increasing deadrise angle β. These figures mean that the impulsive pressure is not occurred at the small deadrise angle $\beta \approx 5$ while the maximum strain is increasing by the large bending moment caused by the impact pressure on the elastic body, especially at St.2.

Validations

The computational conditions in 2D were also similar with experimental conditions. Many SPH particles to represent the elastic rectangular body were used for obtaining information of pressure, stress and strain. In this case, the pressure, stress and strain points are defined into four components that are *xx, xy, yx* and *yy* components.

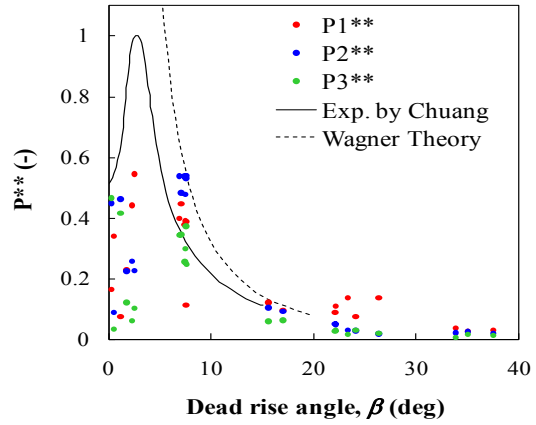

Fig. 4 Relationship between maximum pressure and deadrise angle β

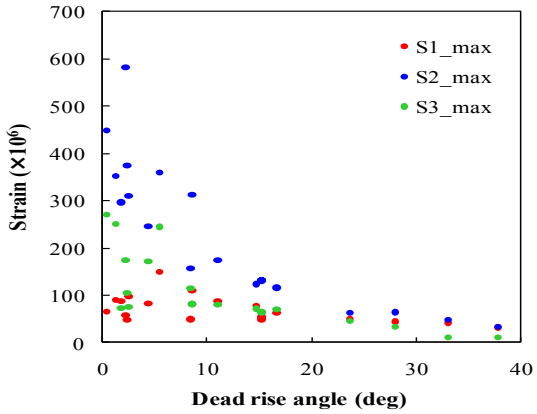

Fig. 5 Relationship between maximum strain and deadrise angle β

The grid size is 2mm and the radius of free surface particle is 0.25mm.The total number of the free surface particle located near the free surface is 6,024. The radius of the SPH particle on the elastic body is 0.25mm and the total number is 3,900 for the elastic body. These conditions are based on our previous numerical research to work well. Time increments are 5.0×10^{-4}sec for liquid phase and 2.5×10^{-5}sec for the elastic body. The density ratio between water and air is 800 and the viscosity ratio is 55 at the initial numerical condition. The numerical model based on multiphase flow formulation can compute directly air cushion effect and air-water interaction due to impact pressure. Young's modulus is 69GPa and Poisson's ratio is 0.35 for elastic ship.

Figure 6 shows one example of time histories of computed strain and stress of the acrylic model in *xx* component for β=2.5°. The *xx* component is measured at middle point S2 of the bottom frame of the body. From this figure, the computational result show fair proportional magnitude between stress and strain.

Figure 7, one example case with β=15°, shows the comparison of time history of strain between computation and experiment at S1, S2 and S3 on the bottom frame of the elastic body. From those figures, computational results have similar tendency with experimental results, and overall of computational results show satisfactory in good agreement with experimental results.

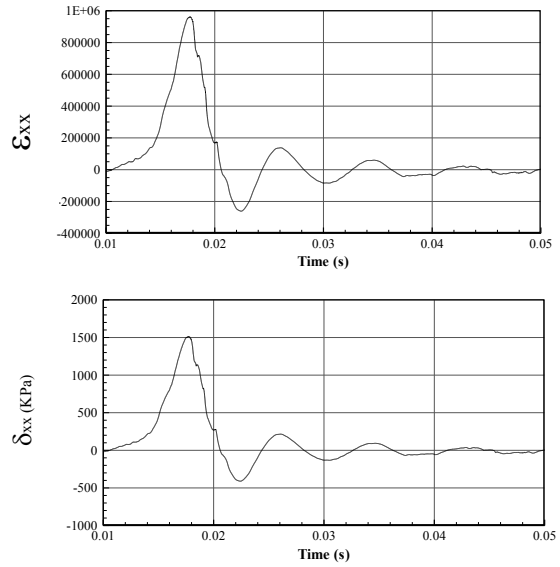

Fig. 6 Time history of computed internal strain and stress in *xx* component (β=2.5°)

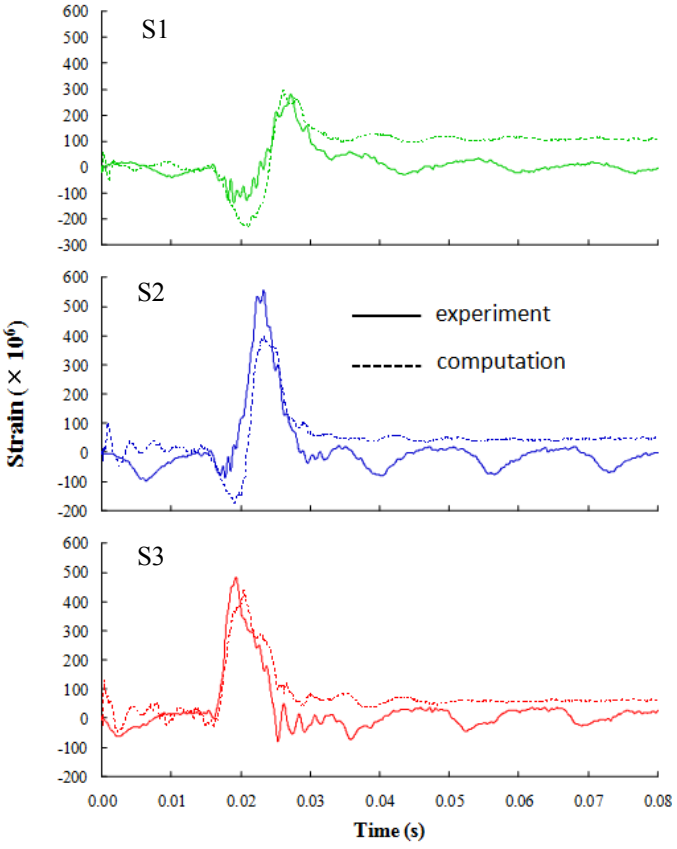

Fig. 7 Comparisons of time history of strain between computation and experiment (deadrise angle β=15°)

Figure 8 shows relationship between the spatial distribution of internal strain of the elastic body and the impact pressure in water during the water entry process. The internal stress and strain are distributed, and the bottom frame of the elastic body is highly deformed

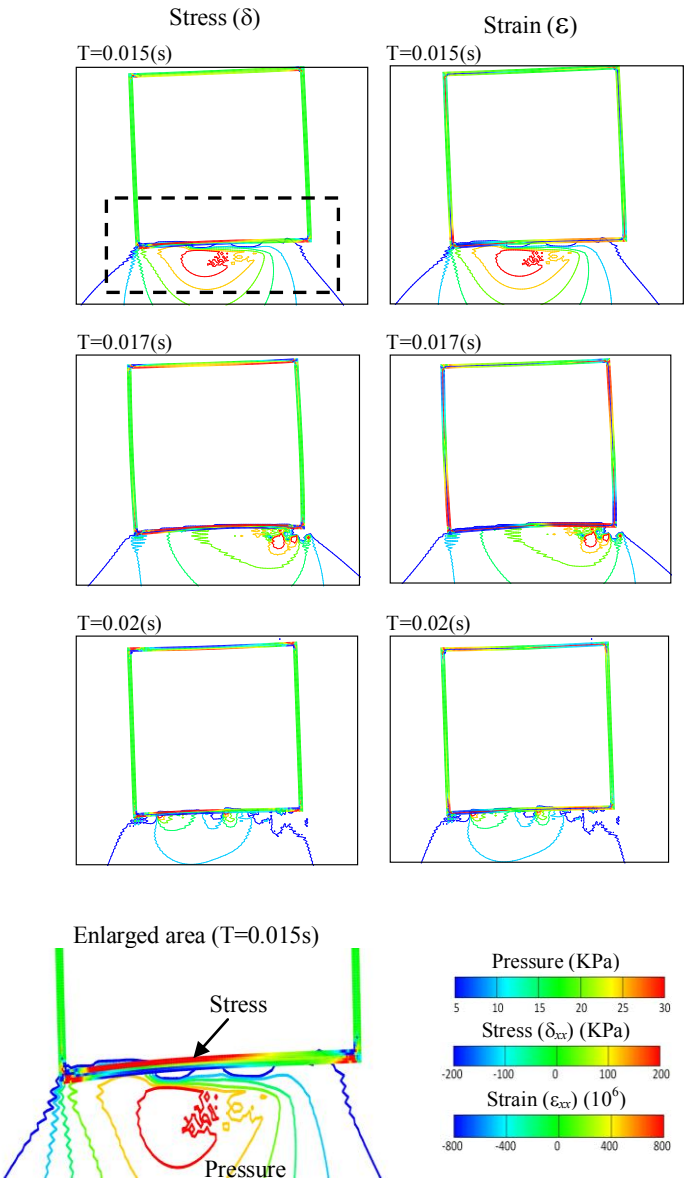

Fig. 8 Internal strain field in elastic body and pressure distribution under the free surface during water entry process (β=2.5°)

at T=0.017, and it is returning gradually to original shape as shown at T=0.02. In the enlarged area, the computed water impact pressure is acting on the bottom frame and then the largely internal strain is occurred at this point.

Application to Hydroelasticity of Ship Slamming in Waves

In this section, hydrodynamic and hydroelastic effects on a ship with elasticity are investigated and this is emphasized to analyze slamming behaviors in waves. In order to investigate the hydrodynamic and hydroelastic effect, our numerical method is applied to ship slamming in heading regular wave and it is also verified and validated in impact pressure and internal strain on a ship with elasticity.

The incident wave height is H_w / L_{pp}=0.06 and the wave length is λ / L_{pp}=1.56, and then ten cases based on wave theory are performed

in numerical water tank.

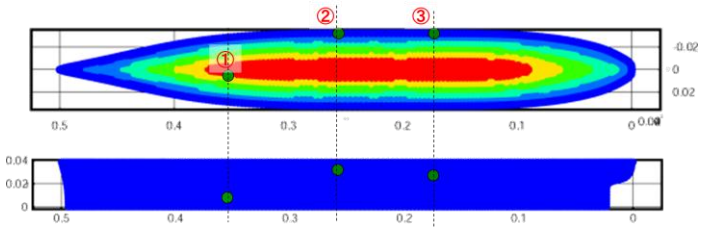

Fig. 9 Location of measurement point of internal strain on elastic ship body

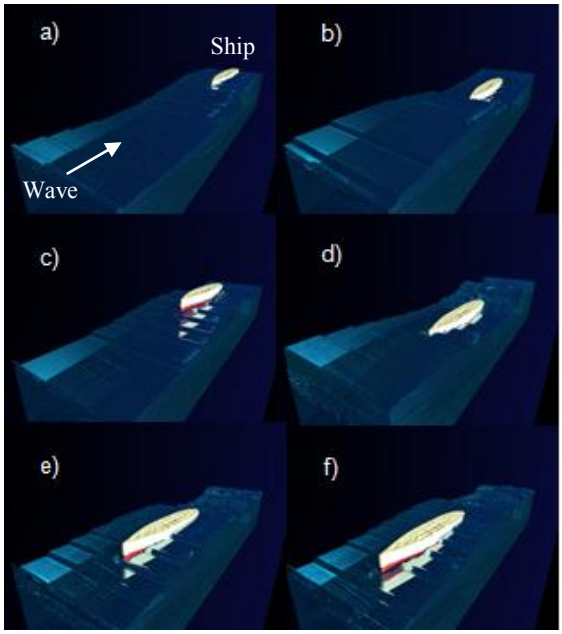

Fig. 10 Snapshots of freely ship motion with hydroelastic behaviors in regular heading wave.

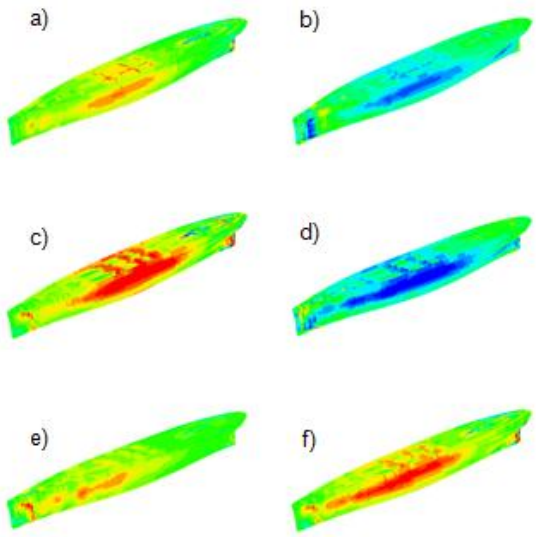

Fig. 11 Internal strain field due to hydroelastic behavior of ship

The periodic boundary in both upstream and downstream is imposed with wave velocity to reduce computational cost. The numerical results during four to six wave periods are used for analysis to avoid several disturbances due to reflection and diffraction wave. The ship speed is 1.0m/sec at the initial condition. The heave and pitch motion are only considered and the other motions are fixed in this case. The grid size is $0.01\,L_{pp}$ and the radius of free surface particles is $0.005\,L_{pp}$. The total number of the free surface particle located near the free surface is 300,000. Its maximum number is one million for the case of long wave period. The radius of the SPH particle is $0.005\,L_{pp}$ and the total number is 18,000 for the ship. These conditions are based on our previous numerical research to work well. Time increments are 10^{-4} sec for liquid phase and 10^{-5}sec for ship, respectively. Fr number and Re number normalized by the ship speed and length are 0.13 and $3.0\text{x}10^{6}$. Young's modulus is 500GPa and Poisson's ratio is 0.3 for the elastic ship. Then, the strain monitoring points represented by SPH particle are located at forward point near the ship bottom (1), centre point near midship (2), and back side of ship (3) as shown in Fig. 9.

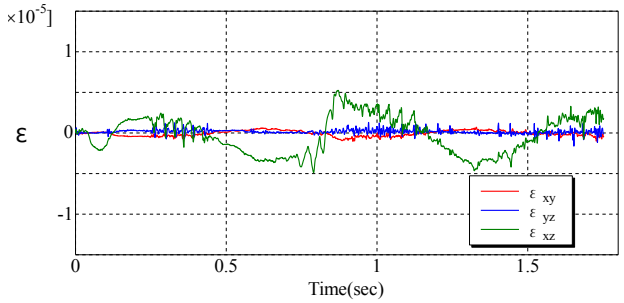

(a) Front point

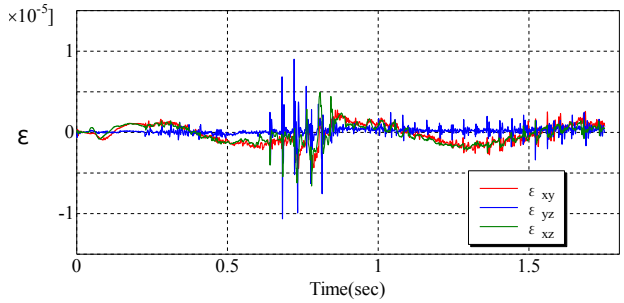

(b) Center point

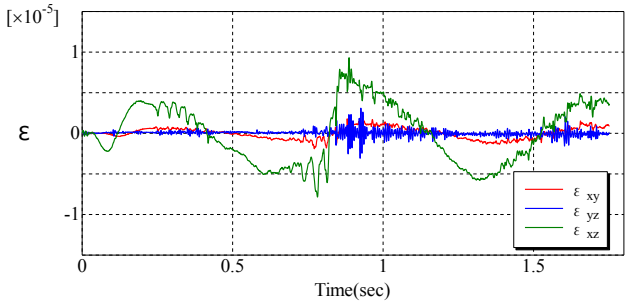

(c) Back point

Fig. 12 Time history of internal strain at each location

Some snapshots of the freely ship motion with hydroelastic behaviors

in waves are shown in Fig.10. Figures 11 shows internal strain distribution acting on each position of the ship based on Fig. 9. The internal strain distribution shows that the elastic ship is deformed by wave force. The repetition of the wave force influences the large variation in the spatial and temporal distribution of the internal strain. In addition, the water impact load effects on the localized large strain distribution. The high strain is occurred when the ship position is in the wave crest whereas negative strain is occurred when it is in the wave trough.

Fig. 12 shows time history of internal strain on three locations. The variation of time series can be found with the wave period (one sec), especially in both the front and back points. However, other components, and large strain fluctuations and wave phase can be seen locally different variations. Then, the combined forces and shock loads caused by the wave affect the hull twisted and deformed locally.

CONCLUSIONS

In this study, the hydrodynamic and hydroelastic effects on a floating body were studied numerically by using the Eulerian scheme with Lagrangian particles we have developed. Our numerical model has been developed to predict and clarify hydrodynamic and hydroelastic effects on floating bodies with free surface flows with wave breaking and splashing. The proposed model could treat and solve simultaneously both nonlinear fluid phenomena and floating body motions with elasticity.

The water entry tests of rectangular bodies with elasticity were computed. The computed internal strain and stress were in good agreement with our experimental results. The time history of strain on the body was in good agreement with our experimental result. The model clarified the relationship between internal strain field of the body and impact pressure during water entry process. Furthermore, we have applied to ship motion with elasticity in waves. The internal strain distribution on elastic ship due to slamming was shown in time and space. Therefore, our numerical can be used for predicting hydroelastic response on an elastic ship in nonlinear wave and to clarify ship slamming behaviors with elasticity in design and analysis field.

In future work, our numerical model should be assessed quantitatively in both reproducibility and validation in ship deformation due to hydroelasticity and motions in waves to utilize as a ship design tool.

REFERENCES

Arai, M. and Miyauchi, T. (1998). "Numerical study of the impact of water on cylindrical shells, considering fluid-structure interactions", *Practical Design of Ship and Mobile Unit*, pp.59-68.

Barraf, D. (1997). "An introduction to physically based modeling,: Rigid body simulationI ~Unconstrained rigid body dynamics~, *SIGGRAPH'97 course note*, D3.

Baso, S., Mutsuda, H., Kurihara, T., Kurokawa, T., Doi, Y. and Shi, J. (2011). "An Eulerian scheme with Lagrangian particles for evaluation of seakeeping performance of a ship in nonlinear wave", *Int J of Offshore and Polar Eng*, ISOPE, in press Vol 21, No 2: ISSN 1053-5381.

Bereznitski, A., Boon, B. and Postnov, V. (2000). "The effect of hydroelasticity on the impact pressure due to bottom slamming on ship structure, *Proc. of 11th International Offshore and Polar Eng Conf,* Seattle, USA, Vol IV, pp.227-283.

Bereznitski, A., Boon, B. and Postnov, V. (2001a). "Hydroelastic formulation in order to achieve more accurate prediction of hydrodynamic loads", *Proc. of 11th International Offshore and Polar Eng Conf,* Stavanger,Norway, ISOPE, Vol. 4, pp.337-342.

Bereznitski, A. and Postnov, V. (2001b). "Hydroelastic model for bottom slamming", *The 8th Int Symp on Practical Design of Ship and Other Floating Structure*, China, Vol. 2, pp.911-917.

Bereznitski, A. and Kaminski, M.L. (2002). "Practical Implications of Hydroelasticiy in Ship Design", *Proc. of 11th Intl Offshore and Polar Eng Conf,* Kitakyushu, Japan, Vol 4, www.isope.org.

Chuang, S.L. (1967). "Experiment on Slamming of Wedge-Shaped Bodies, *J of Ship Research*, 11, pp.190-198.

Deuff, J.B., Oger, G., Doring, M., Alessandrini, B. and Ferrant, P. (2006). "SPH analysis of hydrodynamic impact, including hydrodynamic fluid structure coupling", *Hydro-elasticity in Marine Tech*, pp.131-137.

Eagle, A. and Lewis, R.A. (2003). "A comparison of hydrodynamic impacts prediction methods with two dimensional drop test data", *Marine Struct*, 16, pp.175-182.

Faltinsen, O.M. (1997). "The effect of hydroelasticity on ship slamming", *Phil. Trans. R. Soc.*, 355, pp.575-591.

Faltinsen, O.M. (1998). "Hydroelasticity of high-speed vessels", *Hydroelasticity in Marine Technology, Proc. of the 2nd intl Conf*, pp.1-13.

Faltinsen, O.M. (2001). "Slamming with application to planning vessels, green water loading and sloshing", *hydrodynamics in ship and ocean eng*, pp.27-58.

Germano (1992). "Turbulence: the filtering approach", *Journal of Fluid Mechanics*, Vol.238, pp.325-336.

Gingold, R.A., and Monaghan, J.J. (1977). "Smoothed particle hydrodynamics, theory and application to non-spherical stars, *Mon. Not. Roy. Astr. Soc.*, Vol. 181, pp.375-389.

Greenhow, M. and Lin, W.M. (1983). "Nonlinear free surface effects: experiment and theory", Report No.83-19, Dept. of Ocean Engineering, MIT.

Greenhow, M. (1987). "Water entry into initially calm water", *Appl Ocean Res*, Vol.9, pp.214-223.

Hirt, C.W. and Nichols, B.D. (1981). "Volume of fluid (VOF) method for the dynamics of free boundaries", *J. Comput. Phys.*, 39, pp.201-225.

Kleefsman, K.M.T., Fekken, G. and Veldman, A.E.P.A. (2005). "A Volume-of-Fluid based simulation method for water impact problems, *J of Comput. Phys.*, pp.363-393.

Landrini, M., Colagrossi, A. and Tulin, M.P. (2001). "Numerical studies of wave breaking compared to experimental observations", *Proc. of 4th Num. Towing Tank Sympo.* Humberg (Germany).

Mutsuda, H. and Yasuda, T. (2000). "Numerical simulation of turbulent air-water mixing layer within surf-zone", *Proc. of the 27th Int Conf on Coastal Eng*, pp.755-768.

Mutsuda, H. and Faltinsen, O.M. (2007). "A coupled Eulerian-Lagrangian method for free surface problems", *Proc of Intl Conf on Violent Flow*, pp.227-234.

Mutsuda, H. and Shinkura, Y. and Doi, Y. (2008) "An Eulerian scheme with Lagrangian particles for solving impact pressure caused by wave breaking", *Proc. of the 18th Intl Offshore and Polar Eng Conf*, Vol.3, pp.162-169.

Mutsuda, H. and Doi, Y. (2009a). "Numerical simulation of dynamic response of structure caused by wave impact pressure using an Eulerian scheme with Lagrangian particles, *Proc of the 28th Intl Conf Ocean, Offshore and Arct Eng,* Paper No OMAE2009-79736.

Mutsuda, H and Doi, Y (2009b). "Numerical Simulation of Dynamic Response of Structure Caused By Wave Impact Pressure Using an Eulerian Scheme with Lagrangian Particles, " *Proc of the 28th Intl Conf Ocean, Offshore and Arct Eng,* Hawaii, Paper No OMAE2009-79736.

Mutsuda, H, Shimizu, Y and Doi, Y (2009c). "Numerical Study on Interaction Between Violent Wave and Structure Using SPH," *Particle-Based Methods, Fundamentals and Applications,*

PARTICLES 2009, Barcelona, pp. 266-269

Mutsuda, H, Kurokawa, T, Baso, S and Doi, Y (2010). "Numerical Simulation of Interaction Between Wave and Floating Body Using Eulerian Scheme with Lagrangian Particles," *Proc IV Euro Conf Computat Mech (ECCM2010)*, Paris, CD-Rom.

Ng, C.O. and Kot, S.C. (1992). "Computations of water impact on a two-dimensional flat-bottomed body with a volume-of-fluid method", *Ocean Engng*, 19, pp.377-393.

Oger, G., Doring, M., Alessandrini B., and Ferrant P. (2006). "Two-dimensional SPH simulations of wedge water entries", *J. Comp. Physics,* Vol.213, pp.803-822.

Schumann, C. (1998). "Volume of Fluid Computations of Water Entry of Bow Sections", *Proc. of Euromech.*, pp.274.

Tajima, M. and Yabe, T. (1999). "Simulation on slamming of a vessel by CIP method, *J. of the Phys. Soc. Of Japan*, Vol. 68, No. 8, pp.2576-2584.

Takewaki, H. and Yabe, T. (1987). "Cubic-interpolated pseudo particle (CIP) method application to nonlinear or multi-dimensional problems", *J of Computat Physics*, Vol.70 (1987), pp.355-372.

Von Karman, T. (1929). "The impact of seaplane floats during landing, NACA, TN321, Washington.

Wagner, H. (1932). " Über stoss-und Greitvergänge an der Ober-flache von Flüssigkeiten", *Zeitschr. F. Angrew. Math. Und Mech*., Vol.12, No.4, 1932, pp.193-235

Yabe, T. and Wang, P.Y. (1991). "Unified numerical procedure for compressible and incompressible fluid", *J of the Physical Society of Japan*, Vol.60, No.7 (1991), pp.2105-2108.

Yabe, T., Mizoe, H., Takizawa, K., Moriki, H., Hyo-Nam Im, and Ogata, Y. (2004). "Higher-order scheme with CIP method and adaptive soroban grid towards mesh-free scheme", *J of Computat Physics*, Vol.194, pp.57-77.

Zhao, R. and Faltinsen, O.M. (1993). "Water Entry of two-dimensional bodies", *J. Fluid. Mech.*, Vol. 246, pp.593-612.

Zhao, R., Faltinsen,O.M. and Aarnes, J. (1997). "Water entry of arbitrary two-dimensional sections with and without flow separation", *Proc. of 21st Symp. on Naval hydrod.*, pp.408-423.

Zhao, R. and Faltinsen,O.M. (1998). "Water entry of arbitrary axisymmetric bodies with and without flow separation", *Proc. of 22nd Symp. on Naval hydrod.*, pp.652-664.